

TimeLoc: A Unified End-to-End Framework for Precise Timestamp Localization in Long Videos

Chen-Lin Zhang^{1†*} Lin Sui^{1*} Shuming Liu^{2*} Fangzhou Mu^{3*} Zhangcheng Wang⁴ Bernard Ghanem²
¹ Moonshot AI ² KAUST ³ NVIDIA ⁴ Paradigm Inc

Abstract

Temporal localization in untrimmed videos, which aims to identify specific timestamps, is crucial for video understanding but remains challenging. This task encompasses several subtasks, including temporal action localization, temporal video grounding, moment retrieval, and generic event boundary detection. Existing methods in each subfield are typically designed for specific tasks and lack generalizability across domains. In this paper, we propose **TimeLoc**, a unified end-to-end framework for timestamp localization that can handle multiple tasks. First, our approach employs a simple yet effective one-stage localization model that supports text queries as input and multiple actions as output. Second, we jointly train the video encoder and localization model in an end-to-end manner. To efficiently process long videos, we introduce temporal chunking, enabling the handling of videos with over 30k frames. Third, we find that fine-tuning pre-trained text encoders with a multi-stage training strategy further enhances text-conditioned localization. **TimeLoc** achieves state-of-the-art results across multiple benchmarks: +1.3% and +1.9% mAP over previous best methods on THUMOS14 and EPIC-Kitchens-100, +1.1% on Kinetics-GEBD, +2.94% mAP on QVHighlights, and significant improvements in temporal video grounding (+11.5% on TACoS and +6.7% on Charades-STA under R1@0.5). Our code and checkpoints will be released at <https://github.com/sming256/TimeLoc>.

1. Introduction

In video understanding, many tasks involve localizing actions (*i.e.*, temporal action localization [26, 28, 59]), text descriptions (*i.e.*, temporal sentence grounding [38, 43]), and event boundaries (*i.e.*, generic event boundary detection [22, 42, 65]) by identifying timestamps within an untrimmed video. These *timestamp localization* tasks have attracted growing interest for their many applications in

*Equal contribution.

†Corresponding author: Chen-Lin Zhang <zclnjucs@gmail.com>

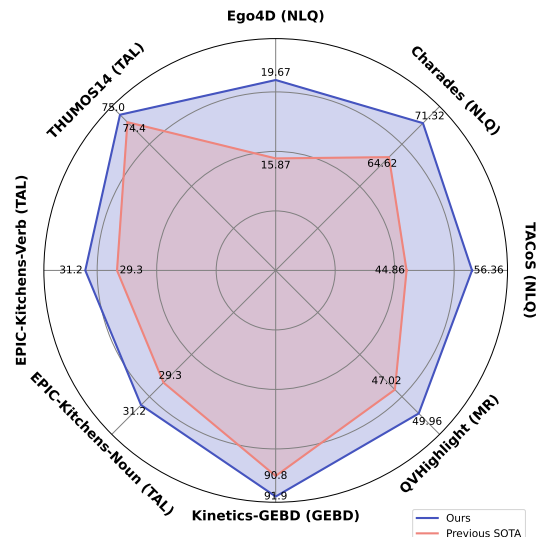


Figure 1. **TimeLoc** achieves state-of-the-art performance across various temporal localization tasks, including temporal action localization, temporal sentence grounding, moment retrieval, and generic event boundary detection.

intelligent personal assistants [16], healthcare [18], and human-robot interaction [12, 67], yet present a significant challenge as they require “finding needles in a haystack” through joint reasoning over spatial, temporal, and textual information.

Although recent advances have led to methods that excel in individual tasks (*e.g.*, [35, 59]), a unified modeling approach that generalizes across the spectrum of timestamp localization tasks is currently lacking, despite their shared problem structure. Moreover, existing methods often train only the localization head(s) on pre-extracted, *frozen* video features, as naively forwarding a full-sized video through a typically large video encoder results in impractical GPU memory usage during gradient updates. However, this prevents the video encoder from adapting to the downstream task, potentially harming model accuracy.

To overcome these challenges, we present **TimeLoc**, a unified framework for Timestamp Localization that supports efficient end-to-end training. **TimeLoc** follows a min-

imalist design that is both simple and effective. *First*, compared to multi-stage approaches like UnLoc [55] and UniVTG [20], TimeLoc features a lightweight one-stage model design that can tackle a broader range of timestamp localization tasks, including generic event boundary detection, while achieving stronger performance. *Second*, given this universal model architecture, we develop a temporal chunking strategy to facilitate the *joint training* of video encoder and localization head(s) on long-form videos, for the first time enabling the processing of over 30K frames on a single GPU. *Third*, on selected tasks with textual inputs, we demonstrate that fine-tuning the pre-trained text encoder following a multi-stage training strategy yields significant performance improvements.

Notwithstanding its simplicity, TimeLoc achieves state-of-the-art (SoTA) accuracy across numerous timestamp localization tasks, as summarized in Figure 1. On *temporal action localization*, it surpasses the previous SoTA method AdaTAD [28] by 1.3% mAP on THUMOS14 [10] and 1.9% mAP on EPIC-Kitchens-100 [5], using the same VideoMAE-L backbone. On *generic event boundary detection*, TimeLoc outperforms EfficientGEBD [65] by 1.1% on Kinetics-GEBD [42]. On *temporal sentence grounding*, TimeLoc demonstrates a significant gain of 8.89% R1@0.3 and 11.5% R1@0.5 on TACoS [38], and an edge of 6.7% R1@0.5 and 6.7% R1@0.7 on Charades-STA [43], when compared to SnAG [35]. On *text-based moment retrieval*, TimeLoc enables an average mAP improvement of 2.94% on QVHighlights [14] over CG-DETR [33].

Our contributions are summarized as follows:

- We propose a unified, end-to-end framework for timestamp localization tasks including temporal action localization, temporal grounding, moment retrieval, and generic event boundary detection. Our framework can be easily extended to include other localization tasks.
- We introduce temporal chunking to facilitate end-to-end training on long videos and find that fine-tuning the text encoder with a multi-stage training strategy further improves the accuracy of text-based timestamp prediction.
- Our framework achieves state-of-the-art performance across a myriad of timestamp localization benchmarks, significantly outperforming previous methods.

2. Related work

2.1. Temporal Video Understanding

Temporal Action Localization aims to identify action instances in untrimmed videos and classify their categories. Methods for this task can be divided into three types: one-stage, two-stage, and DETR-based approaches. One-stage methods, such as ActionFormer [59], TriDet [40], and DyFADet [56], integrate action classification and boundary regression directly using multi-scale feature pyramids. Two-

stage methods incorporate a proposal feature extraction step, exemplified by VSGN [62]’s boundary sampling technique. Recently, end-to-end approaches have emerged [27, 28]. AFSD [19] processes videos at a small spatial resolution for efficient end-to-end learning, while E2E-TAD [29] extensively studies end-to-end training strategies.

Generic Event Boundary Detection (GEBD), introduced by [42], focuses on detecting taxonomy-free event boundaries and segmenting videos into meaningful temporal chunks. Most existing works [46, 65] formulate GEBD as a binary classification problem. DDM-Net [46] constructs a feature bank to store temporal features and captures motion patterns using dense difference maps. EfficientGEBD [65] establishes a strong baseline and utilizes video-domain backbones. A DETR-based detection model was proposed in [45] to address GEBD; however, it was trained offline. Existing GEBD methods are task-specific and lack generalizability across domains.

Temporal Video Grounding localizes moments in untrimmed videos based on text descriptions. Similar to temporal action localization, grounding methods are divided into two-stage and single-stage approaches, focusing on proposal generation and cross-modal fusion. Two-stage methods generate and score temporal segments, with some models conditioning on sentence queries to reduce dense sampling [2, 23, 52–54]. In contrast, single-stage methods localize moments efficiently without explicit proposals, using global features or learnable queries [15, 24, 51, 60, 64]. Despite their efficiency, single-stage methods typically underperform compared to two-stage models on benchmarks. Cross-modal fusion integrates video and text information for improved grounding, evolving from simple late fusion to sophisticated early fusion strategies incorporating LSTMs, GCNs, and memory banks. Recent Transformer-based models [1, 15, 31, 51, 61] leverage early fusion by concatenating video features and text embeddings, enhancing cross-modal reasoning at the cost of increased model complexity. SnAG [35] introduces a scalable single-stage framework that achieves state-of-the-art performance on major benchmarks. However, few works explore end-to-end temporal grounding, and scalability remains an open challenge.

2.2. Efficient End-to-End Fine-tuning

To reduce the cost of applying pre-trained video backbones to downstream tasks, researchers often use offline features as input [21, 35, 59]. AdaTAD [28] demonstrated the benefits of end-to-end (E2E) training for the temporal action localization task and introduced a temporal-informative adapter to reduce the number of trainable parameters. For data-intensive and computationally demanding video understanding tasks, E2E training consumes substantial device memory. To mitigate this, AdaTAD [28] implemented

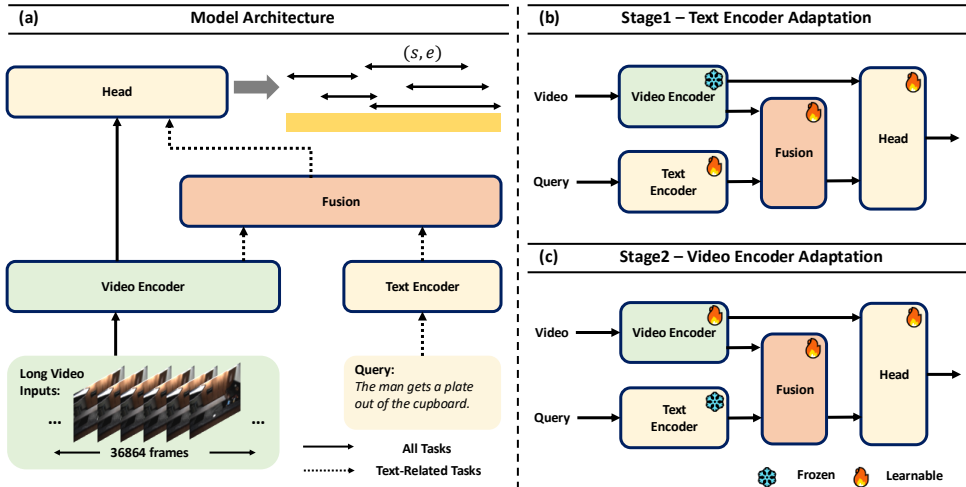


Figure 2. **Pipeline and Multi-Stage Training Strategy of TimeLoc.** (a) The left diagram illustrates our pipeline, which supports temporal localization tasks with or without additional text conditions. The pipeline first extracts features from each modality, applies fusion strategies (if applicable), and then utilizes a lightweight localization head to generate predictions. On the right, the multi-stage training strategy is shown. The training process is divided into two stages: (b) in Stage 1, only the text encoder, fusion module, and localization head are trained. (c) In Stage 2, the text encoder is frozen while the video encoder, fusion module, and localization head are trained.

an alternative adapter placement policy to reduce memory consumption. While parameter-efficient fine-tuning (PEFT) strategies can alleviate memory constraints, they inherently limit the model’s representational capacity. In the development of large language models (LLMs), techniques such as Tensor Parallelism [41] and ZeRO [37] have been employed to distribute resource consumption across multiple devices.

3. Methodology

3.1. Unifying Temporal Localization in Videos

Given an untrimmed video $\mathbf{X} \in \mathbb{R}^{H \times W \times T \times 3}$, where H , W , and T represent the height, width, and duration of the video, many video understanding tasks can be framed as predicting a set of segments $(s_i, e_i, [y_i])_{i=1}^N$, where s_i and e_i denote the start and end timestamps of an event and y_i is an optional label. This formulation unifies different temporal localization tasks:

- **Temporal Action Localization** is a localization task where $y_i \in \{k_1, \dots, k_m\}$, a set of pre-defined actions with m categories.
- **Temporal Video Grounding / Moment Retrieval** requires localizing video segments based on additional textual queries \mathbf{Q} . The query can be a natural language description of an action or a question requiring reasoning over the video content. In these settings, the y_i is empty and the model only needs to generate timestamps.
- **Generic Event Boundary Detection** focuses on identifying temporal boundaries where events transition. We can use these event boundaries $\{b_0, b_1, \dots, b_p\}$ to split the whole video into non-overlapping sequences where $b_0 = 0$ and b_p is the length of the input video. Then the event boundary detection can be converted into timestamp

predictions: $s_i = b_{i-1}$ and $e_i = b_i$.

Building upon the above formulation, the key to unifying these localization tasks lies in designing a *generic localization backbone* that can effectively fuse video with other modalities, along with *flexible localization heads* capable of generating dense timestamps and labels to accommodate varying localization objectives. To this end, we adapt SnAG [35], a one-stage, anchor-free approach as our localization framework. While SnAG was originally developed for video grounding only, we extend it to a broader range of temporal localization tasks with end-to-end training capability.

3.2. One-Stage Localization Framework

As illustrated in Figure 2, our one-stage localization framework consists of a video encoder, a text encoder, a fusion block, and a localization head. Please note that the text encoder and the fusion block are optional. Following [35], this framework maintains a simple yet effective design, enabling the prediction of multi-scale actions and accommodating videos of varying lengths, particularly long-form videos. For more details of the fusion block architecture, we refer the reader to [35].

Next, we present the key modifications introduced in our framework, focusing on three main aspects: video / text feature extraction, the localization head, and the end-to-end training strategy. These enhancements allow the model to generalize across different temporal localization tasks while maintaining efficiency and scalability.

Video Feature Extraction. To encode video frames into compact feature representations, we employ a powerful off-the-shelf video encoder \mathcal{F} , *i.e.*, VideoMAE [47], though

our approach is not limited to this specific model. VideoMAE is pretrained on large-scale video datasets using self-supervised learning followed by supervised fine-tuning, making it well-suited for robust feature extraction.

Specifically, we discard the classification head of VideoMAE, and apply the spatial average pooling after the backbone to obtain the frame-level video representation $f_V \in \mathbb{R}^{C \times T}$, where C is the feature dimension and T is the temporal length. Then, f_V is passed to the subsequent fusion block for temporal modeling with additional text features.

Since VideoMAE operates only on 16-frame inputs, we follow prior work [28] by dividing the video into non-overlapping 16-frame clips. Each clip is independently processed by the encoder, and the extracted features are subsequently aggregated to form the full video representation.

Text Feature Extraction. Similarly, given a text query, we use a text encoder \mathcal{G} to extract the text feature $f_Q \in \mathbb{R}^{C \times L}$, where L is the number of text tokens. In this paper, we explore CLIP and GloVe as text encoders. Then, the video feature f_V and text feature f_Q are fused together by the fusion block to produce the multi-scale feature f_H .

Localization Head. The localization head \mathcal{H} takes as input the video-text fused feature f_H and estimates the start and end offsets $(\Delta s_i, \Delta e_i)$, which represent the relative distances to anchor points or reference timestamps, following an anchor-free approach. It also predicts the confidence score c_i . This formulation enables the model to generalize across different temporal localization tasks while maintaining flexibility in handling task-specific objectives.

Unlike the standard video grounding head in SnAG, our approach also supports a multi-class classification objective, which is essential for temporal action localization tasks. Furthermore, it also supports saliency score prediction for highlight detection, extending the framework to a broader range of temporal localization tasks.

End-to-End Training. Beyond the aforementioned model design, we also jointly fine-tune the video encoder \mathcal{F} along with the fusion block and localization head \mathcal{H} . End-to-end training helps bridge the gap between pretraining and fine-tuning by adapting the model to task-specific data distributions and mitigating domain discrepancies. Moreover, this approach enables the model to learn more robust video representations, reducing the risk of overfitting in the localization head. In our experiments, we find that end-to-end learning is crucial for precise temporal localization, and surprisingly, that a lightweight end-to-end backbone can outperform offline features extracted by gigantic video encoders.

3.3. Handling Long Videos

Our proposed framework effectively performs timestamp localization for most tasks. However, for extremely long videos (*e.g.*, exceeding thirty minutes), we observe that

GPU memory constraints arise, as all video frames must be loaded into memory for end-to-end learning. Detailed ablation studies are provided in Section 4. Previous temporal action localization methods, such as AdaTAD [28], address this issue by freezing the entire backbone and employing ladder networks to reduce memory usage. However, fine-tuning only portions of the video backbone often leads to suboptimal performance and remains insufficient for handling a large number of input frames.

In TimeLoc, inspired by gradient checkpointing [3], we introduce a temporal gradient checkpointing technique into our framework. First, we divide each input video $\mathbf{X} \in \mathbb{R}^{H \times W \times T \times 3}$ into t small temporal chunks along the temporal dimension: Given a partition function $\pi : \{1, 2, \dots, K\} \rightarrow \{1, 2, \dots, t\}$ that maps each index of the third dimension to its corresponding partition, then $\mathcal{K}_p = \{k \in 1, 2, \dots, T\} : \pi(k) = p$ representing the indices of the third dimension that belong to partition p , the divide process can be:

$$\begin{aligned} \mathbf{X}_t &= X_{:, :, \mathcal{K}_p, :}, \\ \mathbf{X} &= \bigcup_{i=1}^t \mathbf{X}_{:, :, \mathcal{K}_p, :}. \end{aligned} \quad (1)$$

For simplicity, we just sequentially divide \mathbf{X} into small chunks. Then, we perform individual forward passes for each chunk \mathbf{X}_i , where $1 \leq i \leq t$, and aggregate the output features into a complete sequence f along the temporal dimension. Importantly, this temporal gradient checkpointing strategy preserves all gradient information, enabling lossless long-video training with reduced peak memory usage at the cost of additional computation time. This approach allows TimeLoc to process nearly arbitrary frame counts, for instance, videos exceeding 36,000 frames.

3.4. Improving Text-Conditioned Timestamp Localization by Fine-Tuning the Text Encoder

Until now, we have maintained the pre-trained text encoder \mathcal{G} unaltered in our framework, with text features f_Q remaining frozen throughout training. Notably, previous research has consistently employed fixed text encoders while tuning video encoders, a practice that warrants further investigation. In our early attempts, fine-tuning both the video and text backbones simultaneously resulted in performance degradation compared to fine-tuning the video backbone alone. This decline likely stems from the modality collision between textual and visual representations.

To address this challenge, we propose a multi-stage training strategy that balances efficiency and effectiveness, as shown in Figure 2 (b) and (c):

- **Stage 1:** Freeze the video backbone \mathcal{F} and fine-tune the text encoder \mathcal{G} , the fusion block, and the localization

head \mathcal{H} . This initial stage introduces negligible computational overhead to the offline training pipeline.

- **Stage 2:** Freeze the text encoder \mathcal{G} , only fine-tune the video backbone \mathcal{F} and remaining components.

Our experiments show that this progressive fine-tuning approach effectively mitigates the modality collision problem, leading to improved performance.

4. Experiments and Analysis

4.1. Experiment Settings

Datasets. We evaluate our proposed method on different localization tasks with the following datasets:

- **THUMOS14** [10] consists of 413 untrimmed videos spanning 20 action categories, with actions ranging from 0.2 to 118 seconds. This dataset is widely used for the temporal action localization task.
- **EPIC-Kitchens 100** [5] contains 700 egocentric videos with various actions. Actions in this dataset are defined by verb-noun combinations.
- **TACoS** [38] is a temporal grounding benchmark consisting of 10.1 hours of cooking videos, with an average of 143.5 queries per video. The dataset exhibits significant variation in video lengths (ranging from 52 seconds to approximately 40 minutes).
- **Charades-STA** [43] consists of videos averaging 30 seconds in length, with each video associated with an average of 2.4 text queries.
- **QVHighlights** [15] includes 10,148 videos and 10,310 text queries. Each video has a maximum duration of 150 seconds. This dataset supports both moment retrieval and highlight detection tasks.
- **Ego4D** [7] is a large-scale collection of egocentric videos capturing daily human activities, encompassing over 3000 hours of content. We conducted experiments with the Ego4D-v1 dataset.
- **Kinetics-GEBD** [42] is a generic event boundary dataset containing 54,691 videos randomly sampled from Kinetics-400 [11], annotated with 1,290,000 generic event temporal boundaries.

Metrics. For temporal action localization tasks, we report the mean Average Precision (mAP) at different temporal Intersection over Union (tIoU) thresholds and the average mAP. Following ActionFormer [59], we evaluate the predictions using tIoU thresholds of $\{0.3, 0.4, 0.5, 0.6, 0.7\}$ on THUMOS14. For EPIC-Kitchens 100, the thresholds are set to $\{0.1, 0.2, 0.3, 0.4, 0.5\}$.

For temporal grounding tasks, we report Recall@ k , where $k \in \{1, 5\}$, at various tIoU thresholds. On the TACoS dataset, the tIoU thresholds are set to $\{0.3, 0.5\}$, while for Charades-STA, we use thresholds of $\{0.5, 0.7\}$.

For moment retrieval tasks, we report the mAP under

tIoU of 0.5 and 0.75, as well as the average mAP with tIoU from 0.5 to 0.95 with 10 steps on QVHighlights.

For generic event boundary detection tasks, we follow prior work [42, 46, 65] and use the Relative Distance (Rel.Dis.) as the evaluation metric. Rel.Dis. quantifies the error between detected and ground truth timestamps, normalized by the length of the action instance. We report F1 scores with Rel.Dis. thresholds ranging from 0.05 to 0.5, as well as the average score for comparative analysis.

4.2. Implementation Details

All experiments are implemented using PyTorch 2.1. By default, we enable memory-efficient techniques such as automatic mixed-precision training and layer-wise gradient activation checkpointing (not to be confused with the proposed temporal gradient checkpointing). We use the AdamW optimizer [32] with a weight decay of 0.05 for all experiments. Unless specifically mentioned, we use spatial resolution 160^2 for VideoMAE, and CLIP [36] as text encoder. For GEBD tasks, we convert the predicted action boundaries (start and end timestamps) into event boundaries.

For task-specific post-processing, we first apply non-maximum suppression (NMS) to all outputs. We select the top- k predictions for most subtasks, including temporal action localization, temporal grounding, and moment retrieval. For GEBD tasks, we directly convert top prediction timestamps into event boundaries, discarding boundaries that are too close. Additional implementation details are provided in the supplementary materials.

4.3. Comparison with SoTA Methods

4.3.1. Temporal Action Localization

THUMOS14. As shown in Table 1, TimeLoc achieves strong performance on THUMOS14, surpassing all previous end-to-end and offline methods. With the VideoMAE-B backbone, TimeLoc outperforms AdaTAD [28] by 0.7% average mAP. However, AdaTAD incorporates additional adapter layers, increasing the model’s capacity. Using the VideoMAE-L backbone (304M), we achieve an average mAP of 75.0%, surpassing the previous best end-to-end method, AdaTAD, by 1.3% under the same backbone and by 0.6% even compared to the VideoMAE-H backbone (633M). This demonstrates that in temporal action localization, efficiently scaling input frames and resolution under end-to-end learning yields better performance than relying on frozen features. For additional results on THUMOS14, please refer to the supplementary materials.

EPIC-Kitchens-100. Table 1 presents our results on EPIC-Kitchens-100. For both verb and noun tasks, TimeLoc, using the VideoMAE-L backbone, achieves significant performance gains over existing methods. With the same backbone as AdaTAD [28], our approach attains an average mAP of 31.2% on the Verb task, surpassing AdaTAD

Table 1. **Temporal Action Localization Results on THUMOS-14 and EPIC-Kitchens 100.** We report mAP% at different tIoUs. E2E means end-to-end training, and Flow refers to offline extracted flow features. Best results are in **bold**, and the second-best results are underlined. † means results were obtained under 224² spatial resolution.

Method	Backbone	E2E	Flow	THUMOS-14							EPIC-Verb					EPIC-Noun					
				0.3	0.4	0.5	0.6	0.7	Avg.	0.1	0.2	0.3	0.4	0.5	Avg.	0.1	0.2	0.3	0.4	0.5	Avg.
ActionFormer [59]	SlowFast-R50	✗	✗	78.7	73.3	65.2	54.6	39.7	62.3	26.6	25.4	24.2	22.3	19.1	23.5	25.2	24.1	22.7	20.5	17.0	21.9
ASL [39]	I3D	✗	✓	83.1	79.0	71.7	59.7	45.8	67.9	27.9	-	25.5	-	19.8	24.6	26.0	-	23.4	-	17.7	22.6
TriDet [40]	I3D	✗	✓	83.6	80.1	72.9	62.4	47.4	69.3	28.6	27.4	26.1	24.2	20.8	25.4	27.4	26.3	24.6	22.2	18.3	23.8
ActionFormer [59]	VideoMAE-L	✗	✓	-	-	-	-	-	-	32.7	31.6	29.1	26.7	<u>23.6</u>	28.7	31.3	29.7	27.2	25.3	21.3	26.9
DyFADet [56]	VideoMAE-g	✗	✓	85.4	-	74.0	-	50.2	71.1	-	-	-	-	-	-	-	-	-	-	-	-
AdaTAD [28]	SlowFast-R50	✓	✗	-	-	-	-	-	-	26.5	25.7	23.9	21.7	17.6	23.1	24.5	23.6	22.3	20.0	16.5	21.4
AdaTAD [28]†	VideoMAE-B	✓	✗	-	-	-	-	-	71.9	-	-	-	-	-	-	-	-	-	-	-	-
AdaTAD [28]	VideoMAE-L	✓	✗	87.7	84.1	76.7	66.4	52.4	73.5	<u>33.1</u>	<u>32.2</u>	<u>30.4</u>	<u>27.5</u>	23.1	<u>29.3</u>	<u>32.4</u>	<u>31.6</u>	<u>30.1</u>	<u>27.4</u>	<u>24.6</u>	<u>29.3</u>
AdaTAD [28]†	VideoMAE-L	✓	✗	-	-	-	-	-	73.7	-	-	-	-	-	-	-	-	-	-	-	-
AdaTAD [28]	VideoMAE-H	✓	✗	88.9	85.3	78.6	66.9	52.5	74.4	-	-	-	-	-	-	-	-	-	-	-	-
TimeLoc	VideoMAE-B	✓	✗	86.1	81.1	74.6	63.3	48.8	70.8	-	-	-	-	-	-	-	-	-	-	-	-
TimeLoc †	VideoMAE-B	✓	✗	87.1	82.8	75.9	63.4	50.6	72.0	-	-	-	-	-	-	-	-	-	-	-	-
TimeLoc	VideoMAE-L	✓	✗	88.8	84.5	77.9	66.8	<u>53.1</u>	74.2	-	-	-	-	-	-	-	-	-	-	-	-
TimeLoc †	VideoMAE-L	✓	✗	89.0	<u>85.0</u>	78.7	68.7	53.5	75.0	34.1	33.3	31.9	29.6	26.8	31.2	35.8	34.4	32.2	29.1	24.6	31.2

Table 2. **Generic Event Boundary Detection Results on Kinetics-GEBD.** Results are obtained under 224² resolution.

Method	Backbone	F1@Rel. Dis.										
		0.05	0.1	0.15	0.2	0.25	0.3	0.35	0.4	0.45	0.5	avg
BMN [21]	ResNet-50	18.6	20.4	21.3	22.0	22.6	23.0	23.3	23.7	23.9	24.1	22.3
BMN-StartEnd [21]	ResNet-50	49.1	58.9	62.7	64.8	66.0	66.8	67.4	67.8	68.1	68.3	64.0
DDM-Net [46]	ResNet-50	76.4	84.3	86.6	88.0	88.7	89.2	89.5	89.8	90.0	90.2	87.3
EfficientGEBD [65]	ResNet-50	78.3	85.1	87.4	88.7	89.6	90.1	90.5	90.8	91.1	91.3	86.6
EfficientGEBD [65]	ir-CSN-152-IG65M	82.9	88.2	90.0	91.1	91.8	92.2	92.5	92.8	93.0	93.2	90.8
TimeLoc	VideoMAE-B-Frozen	77.5	86.0	88.8	90.3	91.3	92.0	92.4	92.7	93.0	93.2	89.7
TimeLoc	VideoMAE-B	82.0	88.6	90.8	92.0	92.8	93.3	93.6	93.9	94.1	94.3	91.5
TimeLoc	VideoMAE-L	<u>82.8</u>	89.1	91.1	92.3	93.0	93.5	93.9	94.2	94.4	94.6	91.9

by 1.9%. Similarly, for the Noun task, our method also achieves an average mAP of 31.2%, outperforming previous state-of-the-art methods, including AdaTAD, by 1.9%. These results further verify the effectiveness of the proposed unified framework under temporal action localization tasks.

4.3.2. Generic Event Boundary Detection

As shown in Table 2, our framework achieves strong performance on generic event boundary detection (GEBD) tasks using the Kinetics-GEBD dataset. Despite its relatively simple design, our method delivers competitive performance compared to approaches specifically designed for GEBD. It also achieves comparable F1 scores with Rel. Dis. @ 0.05. Notably, we observe a 1.1% average F1 score improvement over the previous state-of-the-art method, *i.e.*, EfficientGEBD [65], showing the effectiveness of TimeLoc.

4.3.3. Temporal Grounding and Moment Retrieval

In temporal grounding tasks, our method also demonstrates significant improvements over previous state-of-the-art methods. The results are presented in Table 3 and 4.

TACoS. With the VideoMAE-B backbone, our approach achieves remarkable results with an R1@0.3 of 64.26% and R1@0.5 of 55.79%, outperforming the previous state-of-the-art SnAG (query-centric), which reported an R1@0.3 of 56.44% and R1@0.5 of 44.86%. To conduct a fair compari-

son, we also extracted offline features with the VideoMAE-B backbone and implemented SnAG [35]. Using the same backbones, our proposed method demonstrates R@1 performance gains of 6.05% and 7.78% at tIoU=0.3/0.5 compared to the offline SnAG on the TACoS dataset. These results validate the effectiveness of our proposed end-to-end learning methodology.

Charades-STA. Our method achieves an R1@0.5 of 70.19% and an R1@0.7 of 50.59%, surpassing all existing methods by substantial margins of 5% with the VideoMAE-B backbone. Additionally, there exists a performance gap of 5.51% for R1@0.5 and 6.37% for R1@0.7 between offline SnAG and our method using the same VideoMAE-B backbone. With the more robust VideoMAE-L backbone, our proposed method establishes new state-of-the-art results with R1@0.5 of 71.32% and R1@0.7 of 52.96%.

QVHighlights. As shown in Table 4, most previous methods for moment retrieval rely on pre-extracted features and often ensemble multiple features to achieve stronger performance. However, thanks to our simple localization framework and end-to-end training, TimeLoc achieves an average mAP of 49.96% with the VideoMAE-B, utilizing only 86M parameters. This surpasses the massive InternVideo2 backbone, which has 1B parameters, by a significant margin.

Ego4D-NLQ. On the recently released Ego4D dataset, our

Table 3. **Temporal Grounding Results on TACoS and Charades-STA.** * indicates that pre-extracted VideoMAE-B features are used for SnAG [35]. The best results are in **bold**, while the second-best results are underlined. CLIP is used as the text encoder. † denotes E2E methods with 224 resolution.

Method	TACoS				Charades-STA					
	Backbone	R@1		R@5		Backbone	R@1		R@5	
		0.3	0.5	0.3	0.5		0.5	0.7	0.5	0.7
DRN [58]	C3D	-	23.17	-	33.36	I3D	53.09	31.75	89.06	60.05
CBLN [24]	C3D	38.98	27.65	73.12	46.24	I3D	61.13	38.22	90.33	61.69
CPN [64]	C3D	47.69	36.33	-	-	I3D	51.07	31.54	-	-
DeNet [66]	C3D	-	-	-	-	I3D	59.70	38.52	91.24	66.83
MATN [61]	C3D	48.79	37.57	67.63	57.91	I3D	-	-	-	-
VLG-Net [44]	C3D	45.46	34.19	70.38	56.56	I3D	-	-	-	-
APGN [23]	C3D	40.47	27.86	59.98	47.12	I3D	62.58	38.86	91.24	62.11
IA-Net [25]	C3D	37.91	26.27	57.62	46.39	I3D	61.29	37.91	89.78	62.04
RaNet [6]	C3D	43.34	33.54	67.33	55.09	I3D	60.40	39.65	89.57	64.54
MGSL-Net [25]	C3D	42.54	32.27	63.39	50.13	I3D	63.98	41.03	93.21	63.85
MMN [50]	C3D	39.24	26.17	62.03	47.39	I3D	-	-	-	-
SSRN [68]	C3D	45.10	34.33	65.26	51.85	I3D	65.59	42.65	94.76	65.48
G2L [17]	C3D	42.74	30.95	65.83	49.86	I3D	-	-	-	-
SnAG [35]	C3D	56.44	44.86	81.15	70.66	I3D	64.62	46.26	92.55	71.94
R ² -Tuning [31]	CLIP-B	49.71	38.72	-	-	CLIP-B	59.78	37.02	-	-
BAM-DETR [13]	SF50+CLIP-B	56.69	41.54	-	-	SF50+CLIP-B	59.95	39.38	-	-
SnAG* [35]	VideoMAE-B	58.21	48.01	82.53	72.03	VideoMAE-B	64.68	44.22	90.32	69.19
TimeLoc [†]	VideoMAE-B	64.26	55.79	84.98	77.01	VideoMAE-B	70.19	50.59	91.83	73.04
TimeLoc [†]	VideoMAE-L	65.33	56.36	84.38	76.86	VideoMAE-L	71.32	52.96	93.49	74.44

Table 4. **Moment Retrieval Results on QVHighlights val subset.** * refers to E2E methods with 224 resolution.

Method	Backbone	mAP@0.5	mAP@0.75	Avg. mAP
Moment-DETR [14]	SlowFast+CLIP	-	-	32.20
UniVTG [20]	SlowFast+CLIP	-	-	36.13
QD-DETR [34]	SlowFast+CLIP	62.23	41.82	41.22
EaTR [9]	I3D	61.86	41.91	41.74
CG-DETR [33]	SlowFast+CLIP	65.60	45.70	44.90
CG-DETR [33]	InternVideo2-1B	-	-	<u>47.02</u>
R ² -Tuning [31]	CLIP	69.04	47.56	46.17
BAM-DETR [13]	SlowFast+CLIP	66.33	<u>48.22</u>	46.67
TimeLoc *	VideoMAE-B	<u>67.58</u>	52.20	49.96

method demonstrates substantial improvements over previous state-of-the-art approaches. Using identical backbones (VideoMAE-L and CLIP text encoder), our method achieves 19.67% R1@0.3 and 13.95% R1@0.5, which performs 1.97% better at R1@0.3 and 1.29% better at R1@0.5 compared to our re-implementation of SnAG [35]. TimeLoc also performs better than the recent state-of-the-art methods RGNet [8] with multiple video encoders. Detailed results on Ego4D can be found in supplementary materials.

4.4. Analysis and Findings

In this section, we present ablation studies and additional experiments to demonstrate the key findings of our framework. Unless specified, all experiments are performed on the TACoS dataset under the temporal video grounding task.

Finding 1: End-to-end training and scaling input frames of video encoder significantly enhance performance.

In Tables 5 and 6, we present results with various backbones and input resolutions (both spatial resolution and temporal windows) on the TACoS dataset. All ablation studies are conducted using GloVe-6B as the text feature.

Table 5. **Effectiveness of end-to-end training on TACoS.** E2E refers to end-to-end training of the video encoder. Res. refers to the spatial resolution. GloVe-6B is used to extract text feature.

Video Enc.	E2E	Res.	R1@0.3	R1@0.5
VideoMAE-B	✗	224 ²	58.81	48.01
VideoMAE-B	✓	160 ²	<u>62.18</u>	<u>52.14</u>
VideoMAE-L	✗	224 ²	58.56	48.91
VideoMAE-L	✓	160 ²	63.26	53.49

Table 6. **Impact of scaling model size, spatial resolution and temporal length on TACoS.** For all these experiments in the table, we fix the text encoder.

Video Enc.	Res.	Frames	R1@0.3	R1@0.5
VideoMAE-B	160 ²	18,432	57.79	49.21
VideoMAE-B	160 ²	36,864	62.18	52.14
VideoMAE-B	224 ²	18,432	60.18	51.21
VideoMAE-B	224 ²	36,864	62.68	53.81
VideoMAE-L	224 ²	36,864	63.41	53.86

Table 7. **Impact of different text encoders on TACoS.** Experiments are conducted under the setting of freezing both the text encoder and video encoder.

Video Enc.	Text Enc.	E2E	R1@0.3	R1@0.5
C3D	GloVe-6B	✗	55.76	46.19
C3D	CLIP-B	✗	55.44	45.22
C3D	CLIP-L	✗	55.79	45.14
C3D	BERT-B	✗	56.46	46.64

In Table 5, we conduct comparative analysis between end-to-end training of the video encoder and using frozen features. With the same VideoMAE-B backbone, end-to-end joint training the video encoder can bring significant improvements of 3.37% in R1@0.3 and 4.13% in R1@0.5. These results highlight the enhanced capability of end-to-end training the video encoder to capture complex temporal features, thereby improving overall model accuracy.

Table 6 examines the impact of scaling on the efficacy of the model. By increasing the spatial resolution from 160² to 224² and expanding the number of input frames, we observe considerable performance gains. Notably, the VideoMAE-L backbone exhibits marked improvement at higher resolution and extended temporal length, with R1@0.3 increasing from 57.99% to 63.41%, and R1@0.5 from 49.21% to 53.86%. These findings underscore the importance of both higher resolution and longer temporal sequences for capturing detailed spatial-temporal information essential for model performance. We also present the ablation studies on Charades-STA dataset in the supplementary materials.

Table 8. **Impact of multi-stage training strategy on TACoS.** VideoMAE-B is adopted as the video encoder and 224² is used as spatial resolution of input videos.

Text Enc.	E2E-Text	E2E-Video	R1@0.3	R1@0.5
GloVe-6B	✗	✗	58.21	48.01
GloVe-6B	✗	✓	62.68	53.81
CLIP-B	✗	✗	58.81	49.69
CLIP-B	✓	✗	61.01	51.79
CLIP-B	✗	✓	62.18	52.14
CLIP-B	✓	✓	64.26	55.79
BERT-B	✓	✓	65.21	56.76

Finding 2: Unfreezing text encoder benefits feature fusion, and yields significant performance improvements on text-related tasks.

In Table 7 and Table 8, we observe that merely incorporating more advanced pre-trained text encoders results in minimal performance gains (when using the VideoMAE feature) or even performance degradation (when using the C3D feature). However, when we enable text encoder fine-tuning during the learning process, we observe a substantial performance improvement compared to using fixed text encoders. Table 8 shows that with the original VideoMAE-B feature, fine-tuning the text encoder yields 2.2% and 2.1% improvements on the metrics R1@0.3 and R1@0.5, respectively, comparable to the gains from fine-tuning the video encoders. When fine-tuning both text and video encoders simultaneously, our proposed method achieves better results of 64.26 and 55.79 for R1@0.3 and R1@0.5, respectively. This finding contradicts previous studies by suggesting that offline text features are suboptimal for text-related tasks.

Finding 3: Our multi-stage E2E training strategy unleashes the potential of large pre-trained encoders.

From the results presented in Table 9, we observe that in previous works, larger pre-trained models sometimes exhibit lower performance than smaller ones. This phenomenon may be attributed to the sensitivity of hyper-parameters when training large models. For instance, VideoMAE-L and CLIP-L backbones perform slightly worse than VideoMAE-S/VideoMAE-B + CLIP-B feature combinations. However, within our framework, transitioning to larger pre-trained models yields consistently improved performance. The VideoMAE-B + CLIP-B configuration demonstrates a 2.20% R1@0.3 and 1.88% R1@0.5 performance improvement over VideoMAE-S + CLIP-B under TimeLoc. Furthermore, when employing VideoMAE-L + CLIP-L, we observe an additional 1.07% R1@0.3 and 0.67% R1@0.5 performance gain compared to VideoMAE-B + CLIP-B. These results further validate

Table 9. **Impact of backbone model size on TACoS.** We use 224² as spatial resolution of input videos.

Video Enc.	Text Enc.	E2E	R1@0.3	R1@0.5
VideoMAE-S	CLIP-B	✗	58.39	49.49
VideoMAE-B	CLIP-B	✗	58.81	49.69
VideoMAE-L	CLIP-L	✗	57.29	48.91
VideoMAE-S	CLIP-B	✓	62.06	53.91
VideoMAE-B	CLIP-B	✓	64.26	55.79
VideoMAE-L	CLIP-L	✓	65.33	56.36

Table 10. **Impact of temporal gradient checkpointing (TGC) on memory and speed on TACoS.** Speed refers to the time of one training iteration (forward + backward). OOM means out of memory on H100-80G. Values are obtained under 224² resolution. The input frame number is equal to the window size × 16 frames.

Window Size	Frames	TGC	Memory (GB)	Speed (s/iter)
576	9,216	✗	66.5	5.6
1152	18,432	✗	OOM	-
576	9,216	✓	21.1	6.5
1152	18,432	✓	30.3	13.1
2304	36,864	✓	46.2	26.3

the effectiveness of our proposed TimeLoc approach.

Ablation on memories and speed. We present the training memory requirements and processing speed of TimeLoc on the TACoS dataset. Our analysis reveals that without the proposed temporal gradient checkpointing technique, the temporal length of the input window is limited to 576 (9,216 frames). Expanding the window size to 1152 (18,432 frames) results in out-of-memory errors. However, with temporal gradient checkpointing enabled, our approach supports window sizes of up to 2304 (36,864 frames), with potential for further expansion. Notably, enabling temporal gradient checkpointing incurs training speed penalty. We leave speed optimization in future work.

5. Conclusion

In this paper, we presented TimeLoc, a simple and accurate framework for timestamp localization in videos, including temporal action localization, temporal video grounding, generic event boundary detection, and moment retrieval. To handle long videos efficiently, we introduced temporal gradient checkpointing. Additionally, we discovered that fine-tuning a pre-trained text encoder enhances the performance of text-conditioned timestamp localization. The proposed TimeLoc achieves superior accuracy and efficiency across a range of challenging benchmarks for both short and long videos. We hope our analysis on scaling and model design provides insights into video grounding and, more broadly, scalable video understanding.

References

- [1] Wayner Barrios, Mattia Soldan, Alberto Mario Ceballos-Arroyo, Fabian Caba Heilbron, and Bernard Ghanem. Localizing moments in long video via multimodal guidance. In *ICCV*, 2023. 2
- [2] Shaoxiang Chen and Yu-Gang Jiang. Semantic proposal for activity localization in videos via sentence query. In *AAAI*, 2019. 2
- [3] Tianqi Chen, Bing Xu, Chiyuan Zhang, and Carlos Guestrin. Training deep nets with sublinear memory cost. *arXiv preprint arXiv:1604.06174*, 2016. 4
- [4] Feng Cheng and Gedas Bertasius. Tallformer: Temporal action localization with long-memory transformer. In *ECCV*, 2022. 13
- [5] Dima Damen, Hazel Doughty, Giovanni Maria Farinella, Sanja Fidler, Antonino Furnari, Evangelos Kazakos, Davide Moltisanti, Jonathan Munro, Toby Perrett, Will Price, et al. Scaling egocentric vision: The epic-kitchens dataset. In *ECCV*, 2018. 2, 5
- [6] Jialin Gao, Xin Sun, Mengmeng Xu, Xi Zhou, and Bernard Ghanem. Relation-aware video reading comprehension for temporal language grounding. In *EMNLP*, 2021. 7
- [7] Kristen Grauman, Andrew Westbury, Eugene Byrne, Zachary Chavis, Antonino Furnari, Rohit Girdhar, Jackson Hamburger, Hao Jiang, Miao Liu, Xingyu Liu, et al. Ego4D: Around the world in 3,000 hours of egocentric video. In *CVPR*, 2022. 5
- [8] Tanveer Hannan, Md Mohaiminul Islam, Thomas Seidl, and Gedas Bertasius. RGNet: A unified clip retrieval and grounding network for long videos. In *ECCV*, pages 352–369, 2024. 7, 12
- [9] Jinyun Jang, Jungin Park, Jin Kim, Hyeongjun Kwon, and Kwanghoon Sohn. Knowing where to focus: Event-aware transformer for video grounding. In *Proceedings of the IEEE/CVF International Conference on Computer Vision*, pages 13846–13856, 2023. 7
- [10] YG Jiang, J Liu, A Roshan Zamir, G Toderici, I Laptev, M Shah, and R Sukthankar. Thumos challenge: Action recognition with a large number of classes, 2014. 2, 5
- [11] Will Kay, Joao Carreira, Karen Simonyan, Brian Zhang, Chloe Hillier, Sudheendra Vijayanarasimhan, Fabio Viola, Tim Green, Trevor Back, Paul Natsev, et al. The kinetics human action video dataset. *arXiv preprint arXiv:1705.06950*, 2017. 5
- [12] Tomáš Krajník, Miroslav Kulich, Lenka Mudrová, Rares Ambrus, and Tom Duckett. Where’s waldo at time t? using spatio-temporal models for mobile robot search. In *2015 IEEE International Conference on Robotics and Automation (ICRA)*, pages 2140–2146. IEEE, 2015. 1
- [13] Pilhyeon Lee and Hyeran Byun. BAM-DETR: Boundary-aligned moment detection transformer for temporal sentence grounding in videos. In *ECCV*, pages 220–238, 2024. 7
- [14] Jie Lei, Tamara L Berg, and Mohit Bansal. Detecting moments and highlights in videos via natural language queries. *Advances in Neural Information Processing Systems*, 34: 11846–11858, 2021. 2, 7
- [15] Jie Lei, Tamara L Berg, and Mohit Bansal. Detecting moments and highlights in videos via natural language queries. *NeurIPS*, 2021. 2, 5
- [16] Stan Weixian Lei, Difei Gao, Yuxuan Wang, Dongxing Mao, Zihan Liang, Lingmin Ran, and Mike Zheng Shou. Assistsr: Task-oriented video segment retrieval for personal ai assistant. *arXiv preprint arXiv:2111.15050*, 2021. 1
- [17] Hongxiang Li, Meng Cao, Xuxin Cheng, Yaowei Li, Zhihong Zhu, and Yuexian Zou. G2L: Semantically aligned and uniform video grounding via geodesic and game theory. In *ICCV*, 2023. 7
- [18] Han Liang, Jincai Chen, Fazlullah Khan, Gautam Srivastava, and Jiangfeng Zeng. Audio-visual event localization using multi-task hybrid attention networks for smart healthcare systems. *ACM Transactions on Internet Technology*, 2024. 1
- [19] Chuming Lin, Chengming Xu, Donghao Luo, Yabiao Wang, Ying Tai, Chengjie Wang, Jilin Li, Feiyue Huang, and Yanwei Fu. Learning salient boundary feature for anchor-free temporal action localization. In *CVPR*, 2021. 2, 13
- [20] Kevin Qinghong Lin, Pengchuan Zhang, Joya Chen, Shraman Pramanick, Difei Gao, Alex Jinpeng Wang, Rui Yan, and Mike Zheng Shou. UniVTG: Towards unified video-language temporal grounding. In *ICCV*, 2023. 2, 7
- [21] Tianwei Lin, Xiao Liu, Xin Li, Errui Ding, and Shilei Wen. BMN: Boundary-matching network for temporal action proposal generation. In *ICCV*, pages 3889–3898, 2019. 2, 6
- [22] Tianwei Lin, Xiao Liu, Xin Li, Errui Ding, and Shilei Wen. BMN: boundary-matching network for temporal action proposal generation. In *ICCV*, 2019. 1, 13
- [23] Daizong Liu, Xiaoye Qu, Jianfeng Dong, and Pan Zhou. Adaptive proposal generation network for temporal sentence localization in videos. In *EMNLP*, 2021. 2, 7
- [24] Daizong Liu, Xiaoye Qu, Jianfeng Dong, Pan Zhou, Yu Cheng, Wei Wei, Zichuan Xu, and Yulai Xie. Context-aware biaffine localizing network for temporal sentence grounding. In *CVPR*, 2021. 2, 7
- [25] Daizong Liu, Xiaoye Qu, and Pan Zhou. Progressively guide to attend: An iterative alignment framework for temporal sentence grounding. In *EMNLP*, 2021. 7
- [26] Shuming Liu, Xu Zhao, Haisheng Su, and Zhilan Hu. Tsi: Temporal scale invariant network for action proposal generation. In *ACCV*, 2020. 1
- [27] Shuming Liu, Mengmeng Xu, Chen Zhao, Xu Zhao, and Bernard Ghanem. Etad: Training action detection end to end on a laptop. In *CVPRW*, 2023. 2
- [28] Shuming Liu, Chen-Lin Zhang, Chen Zhao, and Bernard Ghanem. End-to-end temporal action detection with 1b parameters across 1000 frames. In *CVPR*, pages 18591–18601, 2024. 1, 2, 4, 5, 6, 13
- [29] Xiaolong Liu, Song Bai, and Xiang Bai. An empirical study of end-to-end temporal action detection. In *CVPR*, 2022. 2, 13
- [30] Xiaolong Liu, Qimeng Wang, Yao Hu, Xu Tang, Shiwei Zhang, Song Bai, and Xiang Bai. End-to-end temporal action detection with transformer. *IEEE Transactions on Image Processing*, 31:5427–5441, 2022. 13

- [31] Ye Liu, Jixuan He, Wanhua Li, Junsik Kim, Donglai Wei, Hanspeter Pfister, and Chang Wen Chen. R²-Tuning: Efficient image-to-video transfer learning for video temporal grounding. In *ECCV*, pages 421–438. Springer, 2024. 2, 7
- [32] Ilya Loshchilov, Frank Hutter, et al. Fixing weight decay regularization in adam. *arXiv preprint arXiv:1711.05101*, 5: 5, 2017. 5
- [33] WonJun Moon, Sangeek Hyun, SuBeen Lee, and Jae-Pil Heo. Correlation-guided query-dependency calibration for video temporal grounding. *arXiv preprint arXiv:2311.08835*, 2023. 2, 7
- [34] WonJun Moon, Sangeek Hyun, SangUk Park, Dongchan Park, and Jae-Pil Heo. Query-dependent video representation for moment retrieval and highlight detection. In *ICCV*, pages 23023–23033, 2023. 7
- [35] Fangzhou Mu, Sicheng Mo, and Yin Li. SnAG: Scalable and accurate video grounding. In *CVPR*, 2024. 1, 2, 3, 6, 7, 12
- [36] Alec Radford, Jong Wook Kim, Chris Hallacy, Aditya Ramesh, Gabriel Goh, Sandhini Agarwal, Girish Sastry, Amanda Askell, Pamela Mishkin, Jack Clark, et al. Learning transferable visual models from natural language supervision. In *ICML*, 2021. 5
- [37] Samyam Rajbhandari, Jeff Rasley, Olatunji Ruwase, and Yuxiong He. Zero: Memory optimizations toward training trillion parameter models. In *SC20: International Conference for High Performance Computing, Networking, Storage and Analysis*, pages 1–16. IEEE, 2020. 3
- [38] Michaela Regneri, Marcus Rohrbach, Dominikus Wetzel, Stefan Thater, Bernt Schiele, and Manfred Pinkal. Grounding Action Descriptions in Videos. *ACL*, 2013. 1, 2, 5
- [39] Jiayi Shao, Xiaohan Wang, Ruijie Quan, Junjun Zheng, Jiang Yang, and Yi Yang. Action sensitivity learning for temporal action localization. In *ICCV*, 2023. 6, 13
- [40] Dingfeng Shi, Yujie Zhong, Qiong Cao, Lin Ma, Jia Li, and Dacheng Tao. Tridet: Temporal action detection with relative boundary modeling. In *CVPR*, 2023. 2, 6, 13
- [41] Mohammad Shoeybi, Mostofa Patwary, Raul Puri, Patrick LeGresley, Jared Casper, and Bryan Catanzaro. Megatron-lm: Training multi-billion parameter language models using model parallelism. *arXiv preprint arXiv:1909.08053*, 2019. 3
- [42] Mike Zheng Shou, Stan Weixian Lei, Weiyao Wang, Deepti Ghadiyaram, and Matt Feiszli. Generic event boundary detection: A benchmark for event segmentation. In *ICCV*, pages 8075–8084, 2021. 1, 2, 5
- [43] Gunnar A Sigurdsson, Gül Varol, Xiaolong Wang, Ali Farhadi, Ivan Laptev, and Abhinav Gupta. Hollywood in homes: Crowdsourcing data collection for activity understanding. In *ECCV*, 2016. 1, 2, 5
- [44] Mattia Soldan, Mengmeng Xu, Sisi Qu, Jesper Tegner, and Bernard Ghanem. VLG-net: Video-language graph matching network for video grounding. In *ICCVW*, 2021. 7
- [45] Jing Tan, Yuhong Wang, Gangshan Wu, and Limin Wang. Temporal perceiver: A general architecture for arbitrary boundary detection. *IEEE TPAMI*, 45(10):12506–12520, 2023. 2
- [46] Jiaqi Tang, Zhaoyang Liu, Chen Qian, Wayne Wu, and Limin Wang. Progressive attention on multi-level dense difference maps for generic event boundary detection. In *CVPR*, pages 3355–3364, 2022. 2, 5, 6
- [47] Zhan Tong, Yibing Song, Jue Wang, and Limin Wang. Videomae: Masked autoencoders are data-efficient learners for self-supervised video pre-training. In *NeurIPS*, 2022. 3
- [48] Limin Wang, Bingkun Huang, Zhiyu Zhao, Zhan Tong, Yinan He, Yi Wang, Yali Wang, and Yu Qiao. Videomae v2: Scaling video masked autoencoders with dual masking. In *ICCV*, 2023. 13
- [49] Yi Wang, Kunchang Li, Yizhuo Li, Yinan He, Bingkun Huang, Zhiyu Zhao, Hongjie Zhang, Jilan Xu, Yi Liu, Zun Wang, et al. Internvideo: General video foundation models via generative and discriminative learning. *arXiv preprint arXiv:2212.03191*, 2022. 13
- [50] Zhenzhi Wang, Limin Wang, Tao Wu, Tianhao Li, and Gangshan Wu. Negative sample matters: A renaissance of metric learning for temporal grounding. In *AAAI*, 2022. 7
- [51] Sangmin Woo, Jinyoung Park, Inyong Koo, Sumin Lee, Minki Jeong, and Changick Kim. Explore and match: End-to-end video grounding with transformer. *arXiv preprint arXiv:2201.10168*, 2022. 2
- [52] Shaoning Xiao, Long Chen, Jian Shao, Yueting Zhuang, and Jun Xiao. Natural language video localization with learnable moment proposals. In *EMNLP*, 2021. 2
- [53] Shaoning Xiao, Long Chen, Songyang Zhang, Wei Ji, Jian Shao, Lu Ye, and Jun Xiao. Boundary proposal network for two-stage natural language video localization. In *AAAI*, 2021.
- [54] Huijuan Xu, Kun He, Bryan A Plummer, Leonid Sigal, Stan Sclaroff, and Kate Saenko. Multilevel language and vision integration for text-to-clip retrieval. In *AAAI*, 2019. 2
- [55] Shen Yan, Xuehan Xiong, Arsha Nagrai, Anurag Arnab, Zhonghao Wang, Weina Ge, David Ross, and Cordelia Schmid. Unloc: A unified framework for video localization tasks. In *ICCV*, pages 13623–13633, 2023. 2
- [56] Le Yang, Ziwei Zheng, Yizeng Han, Hao Cheng, Shiji Song, Gao Huang, and Fan Li. DyFADet: Dynamic feature aggregation for temporal action detection. In *ECCV*, 2024. 2, 6, 13
- [57] Min Yang, Guo Chen, Yin-Dong Zheng, Tong Lu, and Limin Wang. BasicTad: an astounding rgb-only baseline for temporal action detection. *Computer Vision and Image Understanding*, 232:103692, 2023. 13
- [58] Runhao Zeng, Haoming Xu, Wenbing Huang, Peihao Chen, Mingkui Tan, and Chuang Gan. Dense regression network for video grounding. In *CVPR*, 2020. 7
- [59] Chen-Lin Zhang, Jianxin Wu, and Yin Li. ActionFormer: Localizing moments of actions with transformers. In *ECCV*, 2022. 1, 2, 5, 6, 13
- [60] Hao Zhang, Aixin Sun, Wei Jing, Liangli Zhen, Joey Tianyi Zhou, and Siow Mong Rick Goh. Parallel attention network with sequence matching for video grounding. In *Findings of ACL*, 2021. 2
- [61] Mingxing Zhang, Yang Yang, Xinghan Chen, Yanli Ji, Xing Xu, Jingjing Li, and Heng Tao Shen. Multi-stage aggregated

- transformer network for temporal language localization in videos. In *CVPR*, 2021. [2](#), [7](#)
- [62] Chen Zhao, Ali K Thabet, and Bernard Ghanem. Video self-stitching graph network for temporal action localization. In *ICCV*, 2021. [2](#)
- [63] Chen Zhao, Shuming Liu, Karttikeya Mangalam, and Bernard Ghanem. Re²TAL: Rewiring pretrained video backbones for reversible temporal action localization. In *CVPR*, 2023. [13](#)
- [64] Yang Zhao, Zhou Zhao, Zhu Zhang, and Zhijie Lin. Cascaded prediction network via segment tree for temporal video grounding. In *CVPR*, 2021. [2](#), [7](#)
- [65] Ziwei Zheng, Zechuan Zhang, Yulin Wang, Shiji Song, Gao Huang, and Le Yang. Rethinking the architecture design for efficient generic event boundary detection. In *ACM MM*, pages 1215–1224, 2024. [1](#), [2](#), [5](#), [6](#)
- [66] Hao Zhou, Chongyang Zhang, Yan Luo, Yanjun Chen, and Chuanping Hu. Embracing uncertainty: Decoupling and de-bias for robust temporal grounding. In *CVPR*, 2021. [7](#)
- [67] Yunsong Zhou, Linyan Huang, Qingwen Bu, Jia Zeng, Tianyu Li, Hang Qiu, Hongzi Zhu, Minyi Guo, Yu Qiao, and Hongyang Li. Embodied understanding of driving scenarios. In *ECCV*, pages 129–148. Springer, 2024. [1](#)
- [68] Jiahao Zhu, Daizong Liu, Pan Zhou, Xing Di, Yu Cheng, Song Yang, Wenzheng Xu, Zichuan Xu, Yao Wan, Lichao Sun, et al. Rethinking the video sampling and reasoning strategies for temporal sentence grounding. In *EMNLP Findings*, 2022. [7](#)

6. Appendix

A. More Implementation Details

For the THUMOS14 dataset, we randomly sample a window of 2,304 frames with a temporal stride of 4. For EPIC-Kitchens-100, a window of 18,432 frames is randomly selected with a temporal stride of 2. On both datasets, we set the batch size to 2, and the learning rate of the head to $1e^{-4}$.

For the Kinetics-GEBD dataset, the temporal stride is set to 1, and we set the batch size to 16 and use learning rates of $1e^{-5}$ and $1e^{-3}$ for the video encoder and head, respectively.

For temporal grounding datasets, we extract a window of 2,304 frames with a temporal stride of 4 for Charades-STA and a window of 36,864 frames with a temporal stride of 4 for TACoS and Ego4D. For the QVHighlights dataset, we set the frame rate to 8 FPS and use all available frames (approximately 1,200 frames). The frame resolution is standardized at 160^2 across all experiments. In Stage 1, we set the learning rate ratio of the text encoder to other modules to 1:10 and use a base learning rate of $1e^{-3}$. For Ego4D, we maintain the same learning rate ratio but reduce the base learning rate to $1e^{-4}$. In Stage 2, we freeze the text encoder and transfer its learning rate to the video encoder. We also assign a lower learning rate for the text adapter in the fusion block, specifically $2e^{-5}$ for Ego4D and $2e^{-4}$ for other datasets. In all stages, we use a default batch size of 4. However, for Ego4D, the batch size is set to 2, and for QVHighlights, it is set to 8.

For post-processing, we apply top- k selection followed by SoftNMS and segment voting to refine the predicted segments. We set the top- k value to 100 for temporal grounding and generic event boundary detection, and to 2000 for temporal action localization and highlight detection.

Table 11. Temporal video ground results on Ego4D. [†] means result from SnAG [35].

Video Enc.	Text Enc.	E2E	R1@0.3	R1@0.5
EgoVLP [†]	EgoVLP [†]	✗	15.87	11.26
EgoVLP	EgoVLP	✗	16.58	12.38
CLIP + EgoVLP [8]	CLIP-B	✗	18.28	12.04
VideoMAE-L	CLIP-B	✗	17.70	12.66
VideoMAE-L	CLIP-B	✓	19.67	13.95

Table 12. Multi-stage training strategy on TACoS. Results are obtained under 160^2 resolution.

Backbone	Multi Stage	R1@0.3	R1@0.5
VideoMAE-B	✗	58.76	50.21
VideoMAE-B	✓	64.51	55.76

B. Ablations on Charades-STA

We further present ablation results with different scaling parameters but consistent text encoder configurations on the Charades-STA dataset in Table 13. Despite the distinct characteristics between TACoS (long-duration videos with numerous queries) and Charades-STA (shorter 30-second videos with fewer queries), our proposed method demonstrates similar performance improvements across both datasets. End-to-end training yields approximately 6% performance improvement on R1@0.5 and R1@0.7. Additionally, scaling the spatial resolution and backbone architecture provides a further 1-2% performance enhancement. When utilizing VideoMAE-L as the backbone, we achieve a new state-of-the-art performance with R@1 of 71.32 and 52.96 at tIoU thresholds of 0.5 and 0.7, respectively.

C. Ablations on Ego4D

We also present results on Ego4D-NLQ in Table 11. The original results of SnAG [35] achieve only 15.87% R1@0.3 and 11.26% R1@0.5. For a fair comparison, we first re-implemented SnAG within our framework, obtaining 16.58% R1@0.3 and 12.38% R1@0.5, which is slightly higher than the originally reported results.

Next, we replaced the video backbone with VideoMAE-L and the text encoder with CLIP-B, leading to an additional performance boost of approximately 1% and 0.3%, respectively. TimeLoc further improves upon the offline baseline, achieving gains of 1.97% R1@0.3 and 1.29% R1@0.5. Moreover, TimeLoc outperforms the recent state-of-the-art RGNNet [8], which utilizes two video encoders, further demonstrating the effectiveness of our approach.

D. Ablations on Kinetics-GEBD

In the General Event Boundary Detection task, we also explored the impact of spatial resolution. As shown in Table 14, increasing the resolution from 160^2 to 224^2 only leads to a minor improvement of 0.3 in F1@0.05 and 0.1 in F1@avg, which is significantly smaller than the impact brought by end-to-end training.

Table 13. Ablation studies on Charades-STA. E2E means end-to-end training, and Frozen refers to freezing the backbone during training.

Method	Backbone	E2E	Frozen	Res.	R1@0.5	R1@0.7
SnAG	C3D	✗	✓	224^2	51.75	47.96
SnAG	I3D	✗	✓	224^2	65.19	46.32
TimeLoc	VideoMAE-B	✗	✓	224^2	64.6	44.2
TimeLoc	VideoMAE-B	✓	✓	224^2	67.28	47.2
TimeLoc	VideoMAE-B	✓	✗	224^2	70.19	50.48
TimeLoc	VideoMAE-B	✓	✗	336^2	<u>70.99</u>	<u>52.85</u>
TimeLoc	VideoMAE-L	✓	✗	224^2	71.32	52.96

Table 14. **General Event Boundary Detection Results on Kinetics-GEBD.** Results are obtained under 224² resolution.

Method	Backbone	Res	F1@Rel. Dis.										
			0.05	0.1	0.15	0.2	0.25	0.3	0.35	0.4	0.45	0.5	avg
TimeLoc	VideoMAE-B-Frozen	224 ²	77.5	86.0	88.8	90.3	91.3	92.0	92.4	92.7	93.0	93.2	89.7
TimeLoc	VideoMAE-B	160 ²	81.7	88.4	90.7	91.9	92.7	93.2	93.5	93.8	94.0	94.2	91.4
TimeLoc	VideoMAE-B	224 ²	82.0	88.6	90.8	92.0	92.8	93.3	93.6	93.9	94.1	94.3	91.5

Table 15. Temporal Action Localization Results on the THUMOS14 Dataset. We report mAP (%) at different tIoUs. E2E denotes end-to-end training, while Flow refers to offline extracted optical flow features. The best results are in **bold**, while previous best results are underlined. † indicates results obtained under a 224² spatial resolution.

Method	Backbone	E2E	Flow	THUMOS-14						
				0.3	0.4	0.5	0.6	0.7	Avg.	
BMN [22]	TSN	✗	✓	56.0	47.4	38.8	29.7	20.5	38.5	
TadTR [30]	I3D	✗	✓	62.4	57.4	49.2	37.8	26.3	46.6	
ActionFormer [59]	SlowFast-R50	✗	✗	78.7	73.3	65.2	54.6	39.7	62.3	
ActionFormer [59]	I3D	✗	✓	82.1	77.8	71.0	59.4	43.9	66.8	
ASL [39]	I3D	✗	✓	83.1	79.0	71.7	59.7	45.8	67.9	
TriDet [40]	I3D	✗	✓	83.6	80.1	72.9	62.4	47.4	69.3	
VideoMAEv2 [48]	VideoMAEv2-g	✗	✗	-	-	-	-	-	69.6	
InternVideo [49]	VideoMAE-H*	✗	✗	-	-	-	-	-	<u>71.5</u>	
DyFaNet [56]	VideoMAE-g	✗	✗	84.3	-	73.7	-	50.2	70.5	
DyFaNet [56]	VideoMAE-g	✗	✓	85.4	-	74.0	-	50.2	71.1	
AFSD [19]	I3D	✓	✓	67.3	62.4	55.5	43.7	31.1	52.0	
E2E-TAD [29]	SlowFast-R50	✓	✗	69.4	64.3	56.0	46.4	34.9	54.2	
BasicTAD [57]	SlowOnly-R50	✓	✗	75.5	70.8	63.5	50.9	37.4	59.6	
TALLFormer [4]	VideoSwin-B	✓	✗	76.0	-	63.2	-	34.5	59.2	
Re ² TAL [63]	Re ² VideoSwin-T	✓	✗	77.0	71.5	62.4	49.7	36.3	59.4	
AdaTAD [28]	VideoMAE-B	✓	✗	87.0	82.4	75.3	63.8	49.2	71.5	
AdaTAD [28]†	VideoMAE-B	✓	✗	-	-	-	-	-	71.9	
AdaTAD [28]	VideoMAE-L	✓	✗	87.7	84.1	76.7	66.4	52.4	73.5	
AdaTAD [28]†	VideoMAE-L	✓	✗	-	-	-	-	-	73.7	
AdaTAD [28]	VideoMAE-H	✓	✗	88.9	85.3	78.6	66.9	52.5	74.4	
TimeLoc	VideoMAE-B	✓	✗	86.1	81.1	74.6	63.3	48.8	70.8	
TimeLoc †	VideoMAE-B	✓	✗	87.1	82.8	75.9	63.4	50.6	72.0	
TimeLoc	VideoMAE-L	✓	✗	88.8	84.5	77.9	66.8	<u>53.1</u>	74.2	
TimeLoc †	VideoMAE-L	✓	✗	89.0	85.0	78.7	68.7	53.5	75.0	

incorporate additional optical flow inputs.

E. Ablations on Multi-Stage Training

In Section 3.4 of the main paper, we propose a multi-stage training strategy for fine-tuning the text encoder. Compared to directly performing end-to-end fine-tuning of both the video and text encoders simultaneously, our approach significantly reduces learning difficulty and hyperparameter sensitivity, leading to improved performance.

As shown in Table 12, jointly fine-tuning the video and text encoders achieves only 58.76 R1@0.3 and 50.21 R1@0.5, exhibiting a substantial gap compared to the multi-stage training approach.

F. Additional Results on THUMOS14

In Table 15, we show more results on the THUMOS dataset for comparison. The results demonstrate that TimeLoc achieves state-of-the-art performance compared to both offline and E2E methods, even when some previous methods utilize stronger backbones (e.g., VideoMAE-g) or